

2010-01-2228

COUPLING OF A KERS POWER TRAIN AND A DOWNSIZED 1.2TDI DIESEL OR A 1.6TDI-JI H₂ ENGINE FOR IMPROVED FUEL ECONOMIES IN A COMPACT CAR

Alberto A. Boretti

School of Science and Engineering, University of Ballarat, Ballarat, VIC, Australia

Copyright © 2010 SAE International

ABSTRACT

Recovery of braking energy during driving cycles is the most effective option to improve fuel economy and reduce green house gas (GHG) emissions. Hybrid electric vehicles suffer the disadvantages of the four efficiency reducing transformations in each regenerative braking cycle. Flywheel kinetic energy recovery systems (KERS) may boost this efficiency up to almost double values of about 70% avoiding all four of the efficiency reducing transformations from one form of energy to another and keeping the vehicle's energy in the same form as when the vehicle starts braking when the vehicle is back up to speed. With reference to the baseline configuration with a 1.6 liters engine and no recovery of kinetic energy, introduction of KERS reduces the fuel usage to 3.16 liters per 100 km, corresponding to 82.4 g of CO₂ per km. The 1.6 liters Turbo Direct Injection (TDI) Diesel engine without KERS uses 1.37 MJ per km of fuel energy, reducing with KERS to 1.13 MJ per km. Downsizing the engine to 1.2 liters as permitted by the torque assistance by KERS, the fuel consumption is further reduced to 3.04 liters per 100 km, corresponding to 79.2 g of CO₂ per km and 1.09 MJ per km of fuel energy. These CO₂ and fuel usage values are 11% and 13% better than those of today's highest fuel economy hybrid electric vehicle. The car equipped with a 1.6 liter Turbo Direct Injection Jet Ignition (TDI-JI) H₂ICE engine finally consumes 8.3 g per km of fuel, corresponding to only 0.99 MJ per km of fuel energy.

THE DI-JI ENGINE CONCEPT

The hydrogen fuelled internal combustion engine is now receiving large attention because of the opportunity to operate lean of stoichiometry ($\lambda > 2.25$) achieving top brake efficiencies over 45% while permitting below EURO 6 emissions without any after treatment [1-16]. The Direct Injection jet Ignition engine concept being developed by the Author for gaseous fuels, not only hydrogen but also propane and methane, permits to further boost top brake efficiencies but more than that dramatically increase part load efficiencies controlling the load Diesel like by quantity of fuel injected [11-16].

The Direct Injection Jet Ignition (DI-JI) engine concept uses a jet ignition device to ignite with multiple jets of reacting gases lean stratified mixtures produced within the cylinder by a direct fuel injector. The jet ignition device is made up of a pre-chamber, connected to the main chamber through calibrated orifices, accommodating a pre-chamber fuel injector. The jet ignition device also includes a spark plug or a glow plug according to the spark ignited or auto igniting version. The spark plug ignites a pre-chamber mixture slightly rich. The glow plug controls the auto ignition of a smaller amount of fuel that is injected in the pre-chamber and then auto ignites after impinging on the hot glow plug surface that keeps the temperature within the pre-chamber very high. The hot reacting gases from the pre-chamber then bulk ignite the ultra lean, stratified main chamber mixture through the multiple jets of hot reacting gases entering the cylinder. Fuel is injected directly within the cylinder by the main chamber DI injector operating single or multiple injections to produce a lean stratified mixture. This non homogeneous mixture is mildly lean in an inner region surrounded by air and some residuals from the previous cycle. The extension of the inner region is reduced in size to achieve mean chamber average mixtures ranging from $\lambda = 2.25$ to $\lambda = 7$. This mixture is then ignited by jets of reacting gases that issue from the pre-chamber.

With reference to homogeneous DI or port fuel injection (PFI) and main chamber spark ignition, non homogeneous DI and jet ignition offer the advantage of much faster, more complete, much leaner combustion, less sensitivity to mixture state and composition, and reduced heat losses to the main chamber walls. This is because of better fuel to air ratio of the combusting mixture for same chamber averaged lean conditions, combustion in the bulk of the in cylinder gases, heat transfer cushion of air between hot reacting gases and walls, very high ignition energy, multiple simultaneous ignition sites igniting the bulk of the in cylinder gases, and large concentrations of partially oxidized combustion products initiated in the pre-chamber accelerating the oxidation of fresh reactants.

The concept is an original evolution of the idea of using jet-style ignition to enable the operation of a flame-propagation engine with very lean mixtures explored many times, mostly in the large engine natural gas industry. The major differences of the present concept are the direct injector to the main chamber creating these mixtures from lean homogeneous to lean stratified to explore the many options of low temperature combustion, and the small size pre-chamber fitted with a second fuel injector and a spark or a glow plug, enabling start of combustion by multiple jet of hot reacting gases originating from ignition of a small fraction of the total fuel.

The volume of the jet ignition pre-chamber less than 1 cm^3 is definitively small if compared with main chamber combustion chamber volumes at top dead centre of about 130 cm^3 in a 11 liter in-line 6 truck engines, or about 60 cm^3 in a 3.6 liter V6 passenger car engines, totaling respectively the 0.8 and the 1.6% (indirect injection Diesel engine combustion chambers were not less than 40-50% of the main chamber combustion chamber volumes at top dead centre). This small size volume of the pre-chamber and the requirement to inject within the pre-chamber only a very small fraction of the total fuel is supposed to keep low NO_x production otherwise a major detriment of traditional pre-chamber engines even at very lean operating conditions.

KERS DESCRIPTION

Regenerative braking is probably the best option to improve the fuel economy of passenger cars, light and heavy duty trucks and busses covering driving cycles characterized by frequent accelerations and decelerations [18-33]. Recovering the kinetic energy otherwise lost during braking may indeed significantly reduce the amount of energy to be supplied by the engine to reaccelerate the vehicle.

The latest generation of hybrid electric vehicles (HEV) makes use of many fuel savings technologies to increase fuel efficiency. The power-train system comprises a gasoline engine, an electric motor, a generator, a hybrid battery pack, drive wheels and brakes. The series-parallel power-train system provides drive power independently from the gasoline engine or the electric motor or from both of them simultaneously. Starting is powered by the battery feed electric motor. Normal running with light acceleration is achieved by using a combination of both the battery feed electric motor and the gasoline engine. Full, heavy acceleration is obtained by using all the power of the engine and the battery feed electric motor. During deceleration and braking, the gasoline engine is shut-off and the electric motor convert the kinetic energy into electricity stored in the battery. Finally, stopping, the gasoline engine is also shut-off. The highest fuel economy compact car hybrid electric now available has a CO_2 production of 89 g/km over the new European driving cycle, corresponding to a hydrocarbon fuel economy 10% better than the highest fuel economy vehicle with a traditional power train [17].

The most part of the fuel saving of HEV comes from recharging the battery during braking and using the electric motor to replace the thermal engine power supply, with the latter being shut-off at idle and during braking and portions of the accelerations. Savings also comes in minor part from the thermal engine downsizing permitted by the torque assistance in heavy accelerations. Recovery of kinetic energy in HEV is not very efficient due to a very well known fundamental of physics, that transforming energy from one form to another inevitably introduces significant losses.

When a battery is involved, there are four efficiency reducing transformations in each regenerative braking cycle. (1) Kinetic energy is transformed into electrical energy in a motor/generator, (2) the electrical energy is transformed into chemical energy as the battery charges up, (3) the battery discharges transforming chemical into electrical energy, (4) the electrical energy passes into the motor/generator acting as a motor and is transformed once more into kinetic energy. The four energy transformations reduce the overall level of efficiency. If the motor/generator operates at 80% efficiency under peak load, in and out, and the battery charges and discharges at 75% efficiency at high power, the overall efficiency over a full regenerative cycle is only 36% [29-31]. This means that hybrid vehicles waste near 64% of the braking energy that could possibly be recovered to improve the fuel economy. The ideal solution is to avoid all four of the efficiency reducing transformations from one form of energy to another by keeping the vehicle's energy in the same form as when the vehicle starts braking when the vehicle is back up to speed. This can be done using high-speed flywheels, popular in space and uninterruptible power supplies for computer systems, but novel in ground vehicles. For the space and computer applications, high-speed motor or generators are used to add and remove energy from the flywheels, while in ground vehicles; more efficient mechanical, geared systems are preferred [29-31].

Over the short periods required in cut-and-thrust traffic, a mechanically driven flywheel is much more effective than a battery-based hybrid, providing an overall efficiency over a full regenerative cycle of more than 70%, almost twice the value of battery-based hybrids [29-31]. However, a mechanically driven flywheel system has losses, due to friction in bearings and windage effects, which make it less efficient than a battery-based system in storing energy for long times. Considering the theoretical advantages of storing braking mechanical energy with a much more efficient, simple and lighter mechanical device, and the recent improvements in kinetic energy recovery systems (KERS) for F1 applications [29-31], conventional power-trains with high efficiency Diesel engines may be coupled with KERS to deliver better than hybrids fuel economies.

KERS store energy under vehicle braking and return it under vehicle acceleration. The system utilizes a flywheel as the energy storage device and a Continuously Variable Transmission (CVT) to transfer energy to and from the driveline. Transfer of vehicle

kinetic energy to flywheel kinetic energy reduces the speed of the vehicle and increases the speed of the flywheel. Transfer of flywheel kinetic energy to vehicle kinetic energy reduces the speed of the flywheel and increases the speed of the vehicle. The CVT is used because ratios of vehicle and flywheel speed are different during a braking or acceleration event. A clutch allows disengagement of the flywheel when not used. Recovery of the braking energy reduces the amount of thermal energy requested to power the vehicle and reduce the time the thermal engine is on. Efficiency of KERS energy storage and release, maximum amount of energy being stored, energy loss in start/stop of engine and timing of deceleration and acceleration processes and therefore efficiency of the control play a dominant role in determining the best configuration of a KERS assisted power train. Using optimized strategies, CO₂ and fuel consumption reductions of over 20% are possible on test cycles and more than 30% is possible in real world conditions with gasoline powered vehicles [29-31].

The 60 kW maximum power and 400 kJ energy storage F1 KERS by Flybrid [29-31] has a very light and compact design. It weighs 25 kg and has a volume of 13 litres. The 240 mm diameter flywheel weighs 5 kg and revolves at up to 64,500 rpm. A passenger car KERS has been designed following same concept for an energy capacity of 400 kJ but a maximum power of 30 kW. Weight and dimension are slightly increased to reduce the speed of rotation and account for adoption of a vacuum pump. However, the KERS remain light and compact for easy installation. The efficiency of a round trip regenerative braking is assumed to be 70% [29-31]. This is a minimum value often exceeded during operation [29-31]. Charging and discharging rates are very fast, 50 ms zero to full charge and vice versa. Therefore, the KERS is also quite effective in braking. Control of the coupled regenerative and friction braking is very simple. The KERS is charged during a deceleration and then immediately discharged during the subsequent acceleration. The engine is shut-off during decelerations, and it is restarted during the following acceleration when the kinetic energy recovered during the braking is fully consumed. 70% of the energy needed to brake the vehicle is then used to replace the internal combustion engine supply of energy until fully consumed. Reference values are assumed for energy penalties for start/stop. Results of vehicle simulations are presented in the following section.

FUEL ECONOMY DATA

Fuel economy is measured over test cycles. The ECE+EUDC cycle is a test cycle performed on a chassis dynamometer used for emission certification of light duty vehicles in Europe [EEC Directive 90/C81/01]. The entire cycle includes four ECE segments, repeated without interruption, followed by one EUDC segment. Before the test, the vehicle is allowed to soak for at least 6 hours at a test temperature of 20-30°C. It is then started and the emission sampling begins at the same time. This cold-start procedure is also referred to as the New European Driving Cycle or NEDC. The ECE cycle is an urban driving cycle, also known as UDC. It was devised to represent city driving conditions, e.g. in Paris or Rome. It is characterized by low vehicle speed, low engine load, and low exhaust gas temperature. The EUDC (Extra Urban Driving Cycle) segment has been added after the fourth ECE cycle to account for more aggressive, high speed driving modes. The maximum speed of the EUDC cycle is 120 km/h. Table 1 summarizes the parameters for both the ECE and EUDC cycles.

The highest fuel economy compact car available today [17] couples thermal engine, electric motor, generator, battery pack, drive wheels and brakes to power the vehicle with modulated thermal and electric motors and recovery of braking energy. However, the increase in vehicle weight and dimensions per load volume and the inefficiency of the multiple mechanical to electric energy conversions make their effectiveness much less than what is expected by a car much more environmentally expensive to produce, maintain and dispose.

Table 2 presents fuel economy and CO₂ production data of the highest fuel economy compact car hybrid electric and traditional power train now available [17]. The first has a 1.8 liters gasoline engine, while the second a 1.6 liters TDI Diesel engine. Considered lower heating values (LHV) are 42MJ/Kg and 43.5MJ/Kg for gasoline and Diesel fuels, while densities are 0.75 and 0.835 kg/liter respectively. The hybrid electric vehicle is more environmentally friendly during operation, and in particular covering the urban (cold) sector where accelerations are followed by decelerations and stop thanks to the recovery of braking energy completely dissipated with the traditional power train configuration

Characteristics	ECE	EUDC
Distance [km]	4×1.013=4.052	6.955
Duration [s]	4×195=780	400
Average Speed [km/h]	18.7 (with idling)	62.6
Maximum Speed [km/h]	50	120

Table 1 – Main characteristics of ECE and EUDC cycles.

	highest fuel economy compact hybrid electric car	highest fuel economy compact car with a traditional power train
Fuel	gasoline	Diesel
Urban (cold) Fuel [l/100km]	4	4.7
Extra Urban Fuel [l/100km]	3.8	3.4
Combined Fuel [l/100km]	4	3.8
Combined CO ₂ [g/km]	89	99
Combined Energy [MJ/km]	1.26	1.38

Table 2 – Fuel economy of a compact car with hybrid and traditional power trains.

COMPUTATIONAL RESULTS

A model for the engine and a model for the car have been defined using the WAVE [34] and the Lotus vehicle [35] software. An engine model is applied first to compute the brake specific fuel consumption map versus engine speed and load of the engine. Results of simulations are validated versus available experimental data. Then, a vehicle model is applied to compute the instantaneous fuel flow rate to the engine of the vehicle with traditional power train running a driving cycle. The fuel flow rates are obtained interpolating the brake specific fuel consumption map with the computed instantaneous speeds and loads with corrections for the cold start. Results of simulations are validated versus the fuel consumption data measured.

Table 3 presents the main data of the 1.6 liters TDI Diesel engine, while Table 4 presents the main data of the vehicle. Figure 1 presents the brake specific fuel consumption and the brake efficiency maps computed with WAVE. Brake specific fuel consumptions are in g/kWh and they presented vs. engine speed in rpm and brake mean effective pressure in bar. Brake efficiency is in %. Figure 1 also presents the maximum load brake mean effective pressure vs. engine speed. Load variations are obtained by reducing the amount of fuel injected, i.e. changing the air-to-fuel equivalence ratio. This produces the typical high efficiency map of Diesel over the most part of engine loads. At idle, efficiency theoretically goes to zero, or the brake specific fuel consumption goes theoretically to infinity, because a certain amount of fuel is used to produce an indicated mean effective pressure equal to the friction mean effective pressure with no brake mean effective pressure output. The brake specific fuel consumption map is completed by using finite values at idle.

First, baseline computations have been performed. Results of simulations agree with measured data. Figure 2 presents the engine brake mean effective pressure - speed operating points of the baseline configuration. One operating point is considered every 0.5 s. The baseline 1.6TDI Diesel engine without KERS requires 3.81 liters of Diesel fuel per 100 km. In terms of fuel energy, this solution requires 1.38 MJ/km.

Computations have then been performed modeling a modified version with KERS. The engine is shut-off during decelerations, and it is restarted during the following acceleration when the kinetic energy recovered during the braking is fully consumed. No weight penalty is considered for the KERS, no weight reduction is considered for engine downsizing. 70% of the energy needed to brake the vehicle is then used to replace the internal combustion engine supply of energy until fully consumed. Results show the engine may be stopped more than 50% of the time with KERS, with the engine being run to deliver only the amount of energy needed by the vehicle during part of accelerations and cruising, and to cover the start-stop penalties.

Figure 3 presents the engine brake mean effective pressure - speed operating points of the configuration with a 1.6TDI Diesel engine and the KERS. One operating point is considered every 0.5 s. The shut off of the engine reduces the number of points in figure. The configuration with a 1.6TDI Diesel engine and KERS requires 3.16 liters of Diesel fuel per 100 km. In terms of fuel energy, this solution requires 1.15 MJ/km.

Parameter	1.6 TDI Diesel engine
Number of Cylinders	4
Bore [mm]	79.50
Stroke [mm]	80.50
Compression ratio	16.5
Swept Volume [l]	1.5984

Table 3 – Basic engine data.

Parameter	highest fuel economy compact car with a traditional power train
Weight [kg]	1336
Frontal Area [m ²]	2.2
Drag Coefficient	0.298
Tyre Rolling Radius [m]	0.3080
Final Drive Ratio	3.389
Gearbox	Manual
Number of ratios	5
Gear. 1 Ratio	3.7780
Gear. 2 Ratio	1.9440
Gear. 3 Ratio	1.1850
Gear. 4 Ratio	0.8160
Gear. 5 Ratio	0.6250

Table 4 – Basic vehicle data.

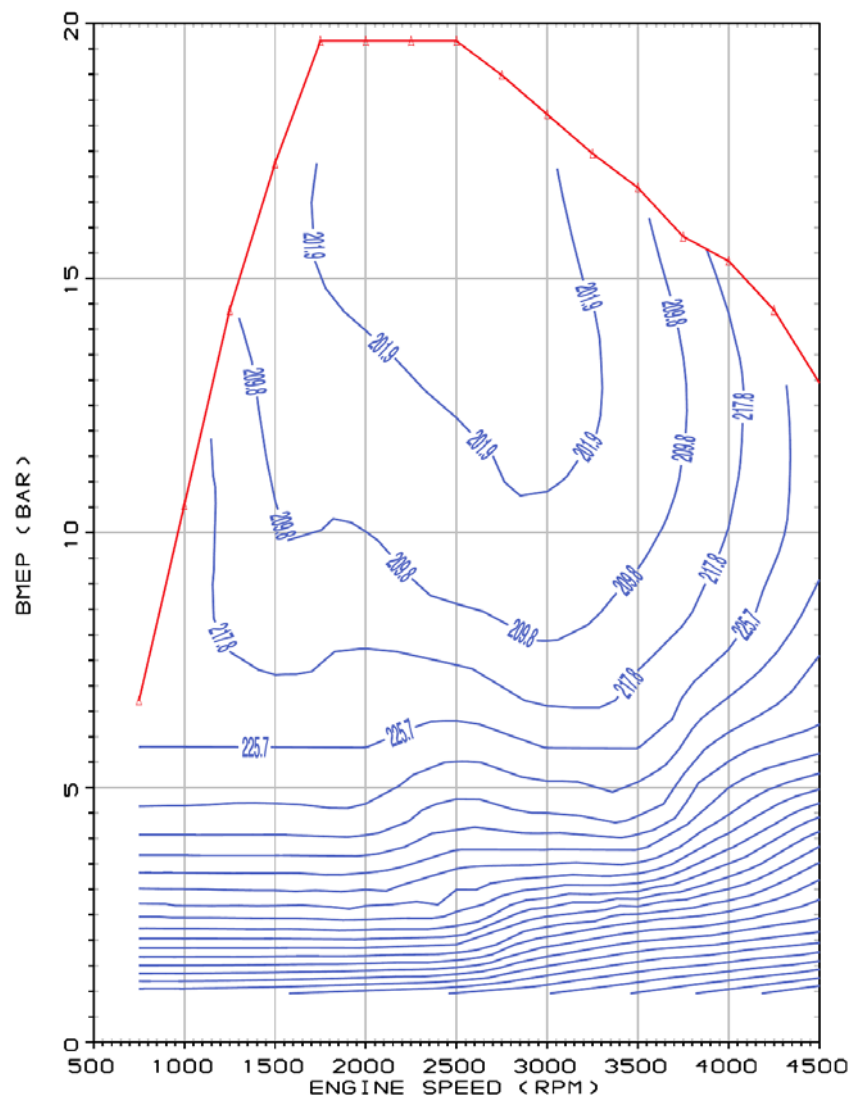


Figure 1.a – Brake specific fuel consumption (in g/kWh) map for the 1.6 TDI Diesel engine.

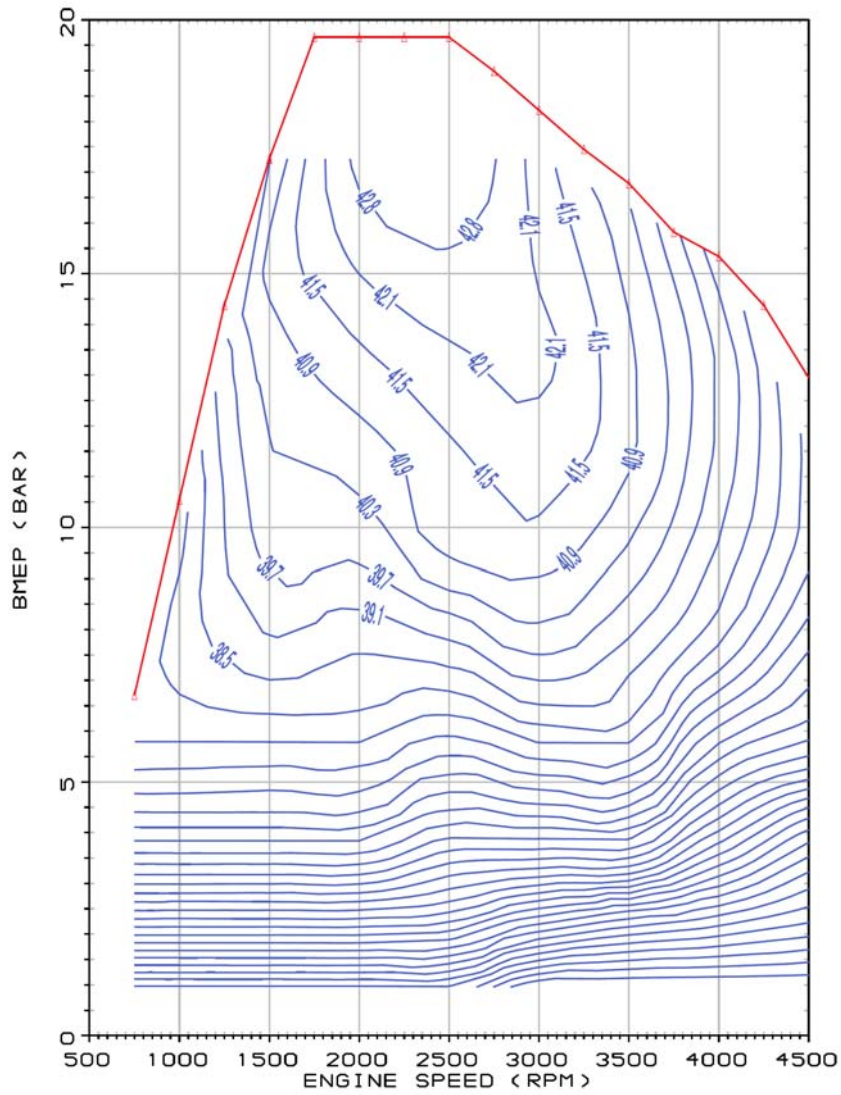


Figure 1.b – Brake efficiency map for the 1.6 TDI Diesel engine.

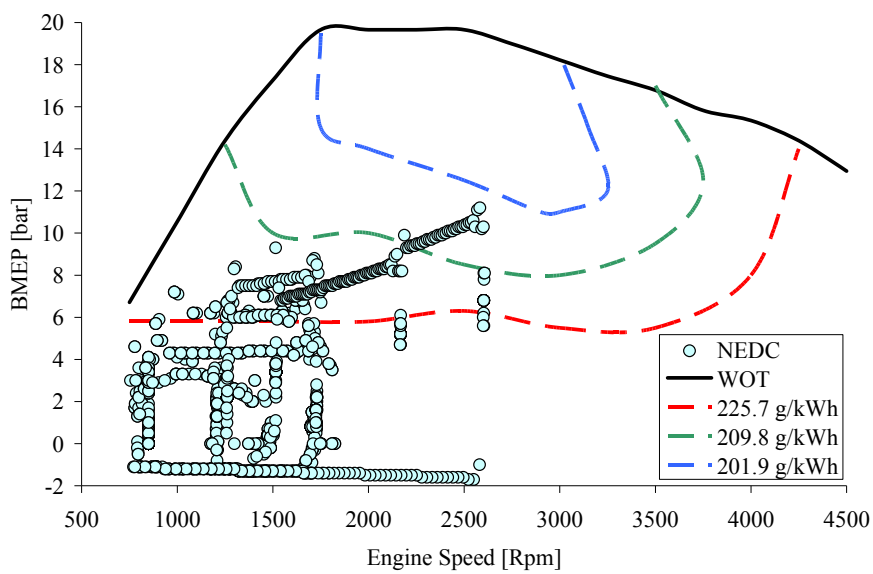


Figure 2 - Engine brake mean effective pressure - speed operating points of the baseline configuration with a 1.6 TDI Diesel engine.

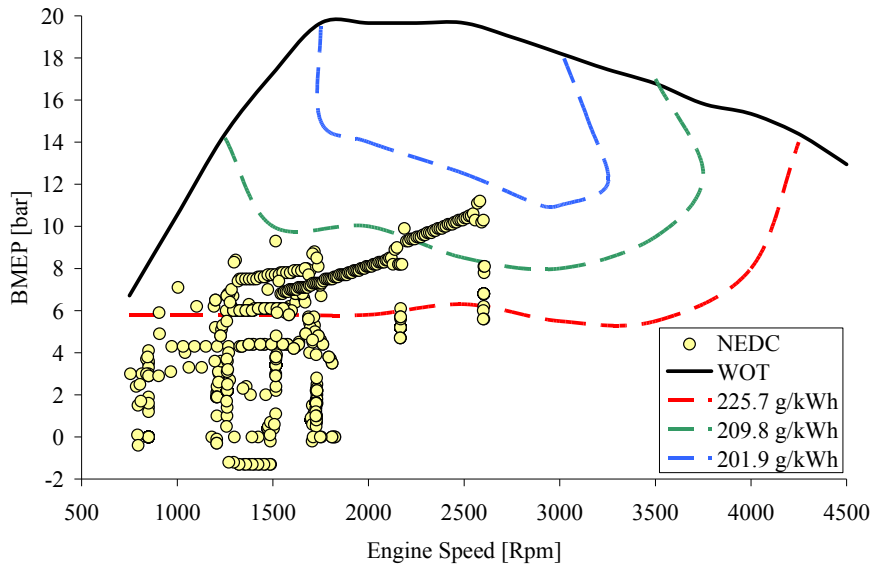


Figure 3 - Engine brake mean effective pressure - speed operating points of the configuration with a 1.6 TDI Diesel engine and KERS.

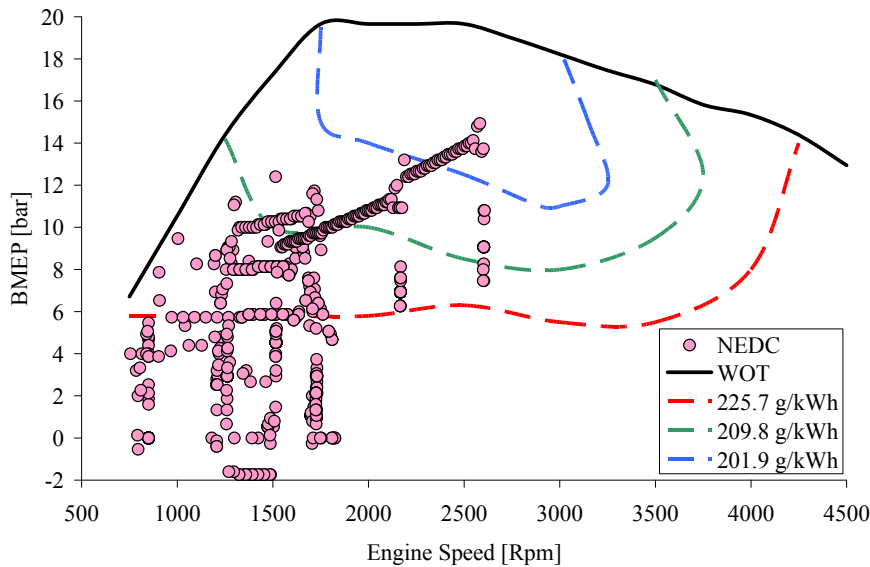


Figure 4 - Engine brake mean effective pressure - speed operating points of the configuration with a 1.2 TDI Diesel engine and KERS.

Computations have finally been performed considering the option to downsize the engine to 1.2 liters thanks to the boost provided by KERS. For sake of simplicity, the same brake specific fuel consumption map and maximum load brake mean effective pressure curve is supposed to apply for a downsized version of the engine to 1.2 liters, having reduced bore and stroke reduced (72.2 and 73.1 mm respectively) and same compression ratio. The turbocharger is also supposed to be properly downsized. Therefore maximum power and maximum torque speeds are the same for both engines, while maximum power and maximum torque outputs reduce with downsizing by the displacement ratio.

Figure 4 presents the engine brake mean effective pressure - speed operating points of the configuration with a 1.2 TDI Diesel engine and the KERS. One operating point is considered every 0.5 s. The shut off of the engine reduces the number of points in figure. The downsizing of the engine increases the operating BMEP towards points of better fuel economy. Torque assistance by KERS permits same maximum accelerations of the larger engine following a deceleration. The configuration with the downsized 1.2 TDI Diesel engine and no KERS has a fuel consumption of 3.66 liters of Diesel fuel per 100 km, corresponding to 1.33 MJ/km of fuel energy. The configuration with the downsized 1.2 TDI Diesel engine and KERS has a fuel consumption of 3.04 liters of Diesel fuel per 100 km. In terms of fuel energy, this solution requires 1.10 MJ/km of fuel energy.

Computations have then been performed for a 1.6 liter H₂ICE engine, derived from the engine in table 3 reducing the compression ratio to 14.5 and adopting a central direct injector plus the central jet ignition pre-chamber. Figure 5 presents the brake specific fuel

consumption and the brake efficiency maps computed with WAVE. Brake specific fuel consumptions are in g/kWh and they presented vs. engine speed in rpm and brake mean effective pressure in bar. Brake efficiency is in %. Figure 5 also presents the maximum load brake mean effective pressure vs. engine speed. Load variations are obtained Diesel-like by reducing the amount of fuel injected, i.e. changing the air-to-fuel equivalence ratio, thanks to the always lean burn properties of the direct injection jet ignition engine.

It has to be pointed out that the conversion to hydrogen is not optimal, and better top brake efficiencies may certainly follow an engine optimization for hydrogen. Despite of that, the hydrogen engine has better than Diesel part load conditions, thanks to the always lean burn properties of the DI-JI engine concept. Figure 6 presents the engine brake mean effective pressure - speed operating points of the configuration with a 1.6 H₂ICE engine and the KERS. The KERS is also used to boost acceleration increasing the engine BMEP when needed in a few points in the low speed range. The 1.6 H₂ICE and KERS reduces the fuel usage to 8 g/km of hydrogen fuel, corresponding to only 0.96 MJ/km of fuel energy.

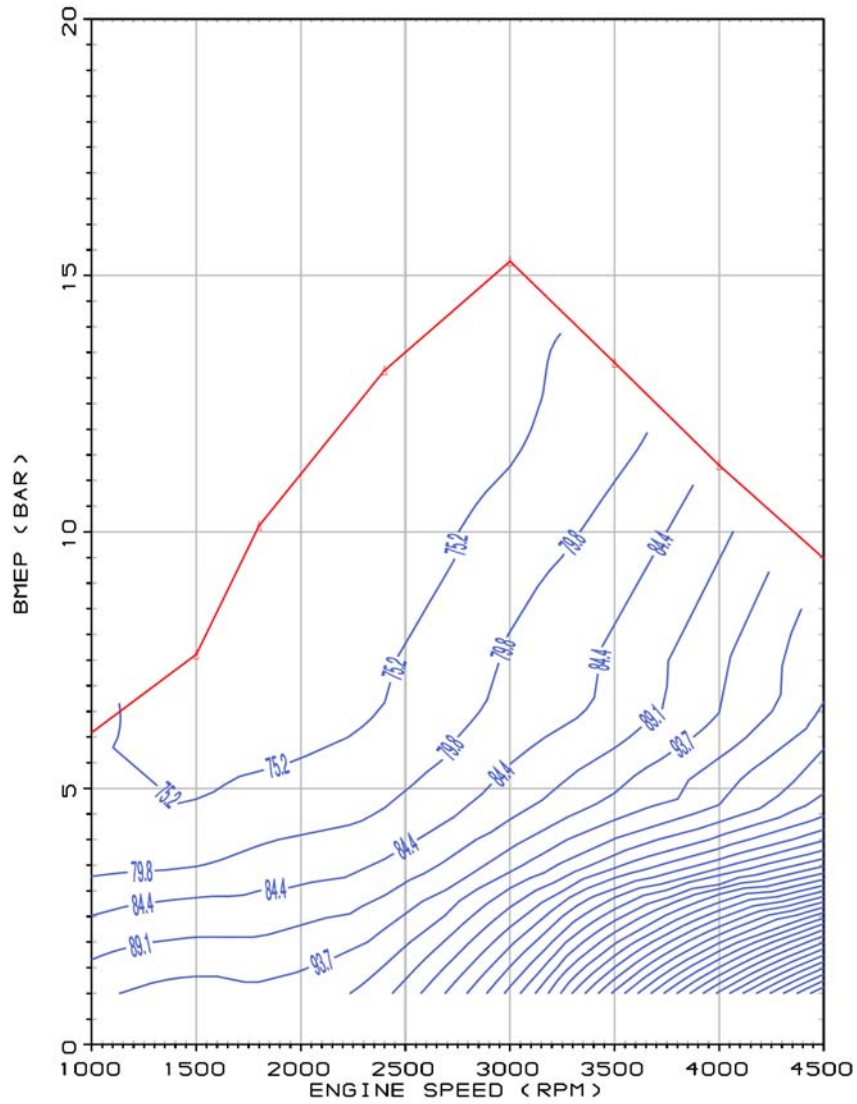


Figure 5.a – Brake specific fuel consumption (in g/kWh) map for the 1.6 H₂ICE engine.

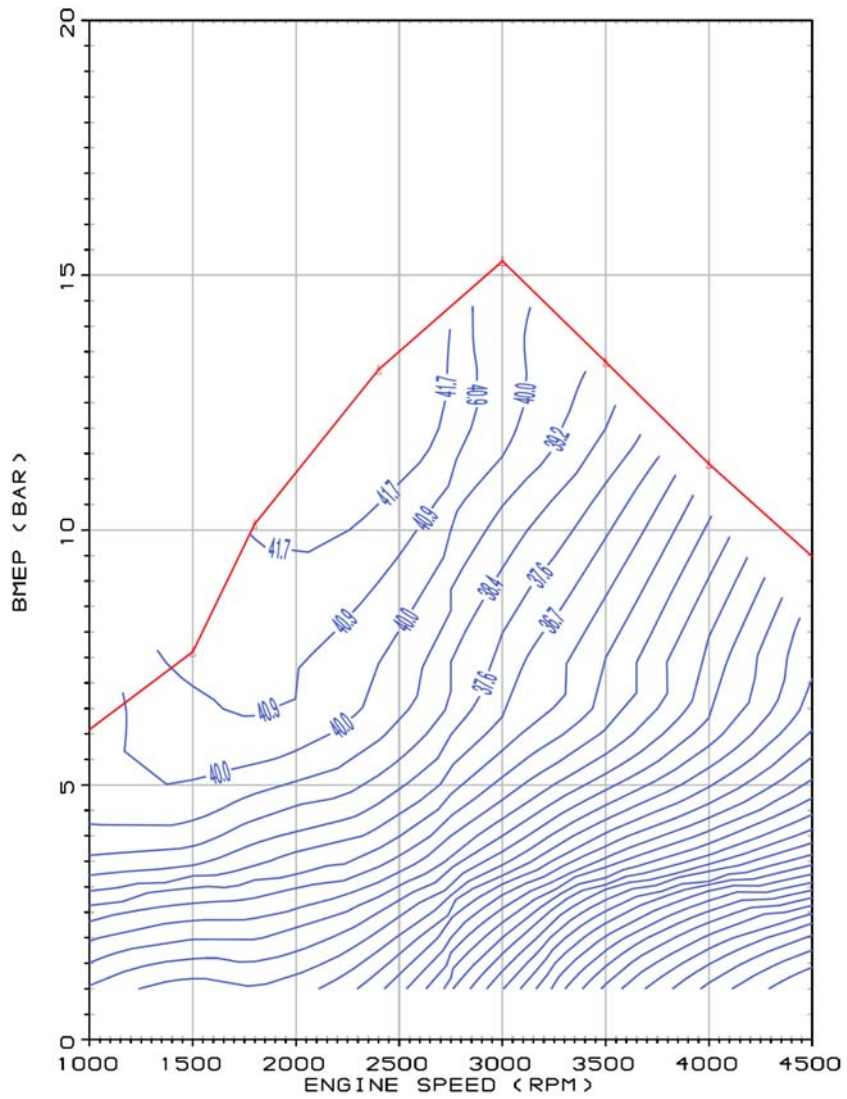


Figure 5.b – Brake efficiency map for the 1.6 H₂ICE engine.

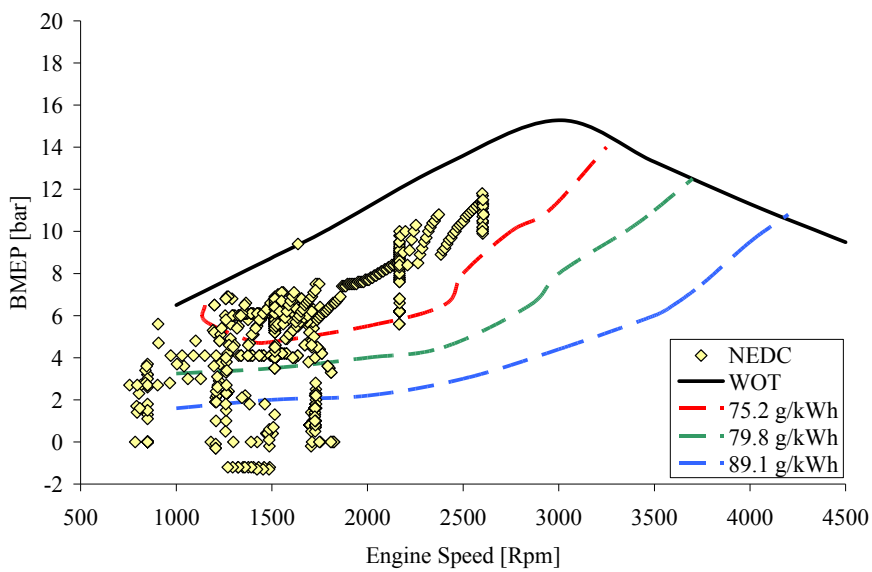


Figure 6 - Engine brake mean effective pressure - speed operating points of the configuration with a 1.6 H₂ICE engine and KERS.

CONCLUSIONS

KERS permit efficient regenerative braking and torque assistance as a means of dramatically improving efficiency and hence reducing fuel consumption and CO₂ emissions, while Direct Injection and Jet Ignition permits not only large top brake efficiencies, but especially very large part load efficiencies.

Computational results presented here for a conventional compact car vehicle originally equipped with a 1.6 TDI Diesel engine running the new European driving cycle (NEDC). Simulations have been performed for the baseline configuration with the 1.6 TDI Diesel engine and no KERS, with same engine and KERS, with a downsized 1.2 TDI Diesel engine and no KERS, with the downsized 1.2 TDI engine and KERS and finally with a 1.6 H₂ICE and KERS. Table 5 below summarizes the fuel economy results of all the modeled configurations.

Configuration	Fuel	Fuel [l/ 100km]	CO ₂ [g/km]	Energy [MJ/ km]
1.6 TDI Diesel	Diesel	3.81	99.2	1.38
1.6 TDI Diesel + KERS	Diesel	3.16	82.4	1.15
1.2 TDI Diesel	Diesel	3.66	95.4	1.33
1.2 TDI Diesel + KERS	Diesel	3.04	79.2	1.10
1.2 H ₂ ICE + KERS	Hydrogen			0.99

Table 5 – Fuel economy of a compact car with and without KERS and different engine solutions.

The car equipped with a 1.2 liter TDI Diesel engine and KERS consumes 25 g/km of fuel producing 79.2 g/km of CO₂ using 1.09 MJ/km of fuel energy. These CO₂ and fuel energy values are more than 10% better than those of today's highest fuel economy hybrid electric vehicle. The fuel energy usage is only 1.10 MJ/km. Adoption of KERS and engine downsizing enables reduction in fuel consumption of nearly 30% and same reductions in CO₂ production when using hydrocarbon fuels.

H₂ICE are able to deliver not only similar to Diesel top brake efficiencies, but also better than Diesel part load efficiencies. The car equipped with a 1.6 liter DI-JI H₂ICE engine and KERS consumes only 8.3 g/km of fuel, corresponding to only 0.99 MJ/km of fuel energy. Hydrogen fuel produced with renewable energy may therefore be used very efficiently in passenger cars equipped with a KERS and having the H₂ICE developed following the direct injection jet ignition concept.

REFERENCES

1. C.M. White, R.R. Steeper, A.E. Lutz, "The hydrogen-fueled internal combustion engine: a technical review", International Journal of Hydrogen Energy, Volume 31, Issue 10, August 2006, Pages 1292-1305.
2. Vincent Knop, Adlène Benkenida, Stéphane Jay, Olivier Colin, "Modelling of combustion and nitrogen oxide formation in hydrogen-fuelled internal combustion engines within a 3D CFD code", International Journal of Hydrogen Energy, Volume 33, Issue 19, October 2008, Pages 5083-509.
3. S. Verhelst, P. Maesschalck, N. Rombaut, R. Sierens, "Increasing the power output of hydrogen internal combustion engines by means of supercharging and exhaust gas recirculation", International Journal of Hydrogen Energy, Volume 34, Issue 10, May 2009, Pages 4406-4412.
4. Ali Mohammadi, Masahiro Shioji, Yasuyuki Nakai, Wataru Ishikura, Eizo Tabo, "Performance and combustion characteristics of a direct injection SI hydrogen engine", International Journal of Hydrogen Energy, Volume 32, Issue 2, February 2007, Pages 296-304.
5. Alberto A. Boretti, Harry C. Watson, "Enhanced combustion by jet ignition in a turbocharged cryogenic port fuel injected hydrogen engine", International Journal of Hydrogen Energy, Volume 34, Issue 5, March 2009, Pages 2511-2516.
6. H. Safari, S.A. Jazayeri, R. Ebrahimi, "Potentials of NOx emission reduction methods in SI hydrogen engines: Simulation study", International Journal of Hydrogen Energy, Volume 34, Issue 2, January 2009, Pages 1015-1025.
7. Gianluca D'Errico, Angelo Onorati, Simon Ellgas, "1D thermo-fluid dynamic modelling of an S.I. single-cylinder H2 engine with cryogenic port injection", International Journal of Hydrogen Energy, Volume 33, Issue 20, October 2008, Pages 5829-5841.
8. Nobuyuki Kawahara, Eiji Tomita, "Visualization of auto-ignition and pressure wave during knocking in a hydrogen spark-ignition engine", International Journal of Hydrogen Energy, Volume 34, Issue 7, April 2009, Pages 3156-3163.
9. J.M. Gomes Antunes, R. Mikalsen, A.P. Roskilly, "An experimental study of a direct injection compression ignition hydrogen engine", International Journal of Hydrogen Energy, Volume 34, Issue 15, August 2009, Pages 6516-6522.
10. Jonathan Nieminen, Ninochka D'Souza, Ibrahim Dincer, "Comparative combustion characteristics of gasoline and hydrogen fuelled ICES", International Journal of Hydrogen Energy, In Press, Corrected Proof, Available online 2 October 2009.

11. A. A. Boretti, H. C. Watson, "*The lean burn direct-injection jet-ignition turbocharged liquid phase LPG engine*", paper presented to the 15th Asia Pacific Automotive Engineering Conference (APAC-15), Hanoi, Vietnam, October 2009.
12. A. A. Boretti, H. C. Watson, "*The lean burn direct-injection jet-ignition gas engine*", International Journal of Hydrogen Energy, Volume 34, Issue 18, September 2009, Pages 7835-7841. DOI:10.1016/j.ijhydene.2009.07.022.
13. A. A. Boretti, H. C. Watson, "*The lean burn direct-injection jet-ignition flexi gas fuel LPG/CNG engine*", paper presented to the 2009 SAE Power trains, Fuels and Lubricants Meeting, San Antonio, Texas, USA, November 2009. SAE P. 2009-01-2790.
14. A. A. Boretti, H. C. Watson, A. Tempia, "*Computational analysis of the lean burn direct-injection jet-ignition hydrogen engine*", Proceedings of the Institution of Mechanical Engineers, Part D: Journal of Automobile Engineering, Volume 224, Number 2/2009, pages 261-269. doi: 10.1243/09544070jauto1278, ISSN: 0954-4070 (Print) 2041-2991 (Online).
15. Alberto A. Boretti, "*Modelling auto ignition of hydrogen in a jet ignition pre-chamber*", International Journal of Hydrogen Energy (2010), doi:10.1016/j.ijhydene.2010.01.114
16. Alberto A. Boretti, "*Vehicle driving cycle performance of the spark-less DI-JI hydrogen engine*", International Journal of Hydrogen Energy (2010), doi:10.1016/j.ijhydene.2010.02.136.
17. <http://www.vcacarfueldata.org.uk> (retrieved July 21, 2010).
18. Ryoji Kasama, Shotaro Naito, Hiroshi Katada, Takanori Shibata, "*The Efficiency Improvement of Electric Vehicles By Regenerative Braking*", SAE P. 780291.
19. Simon Slutsky, Enrico Levi, "*Regenerative Braking in Diesel-Powered Urban Buses*", SAE P. 841690.
20. Floyd A. Wyczalek, Tsih C. Wang, "*Regenerative Braking Concepts for Electric Vehicles--A Primer*", SAE P. 920648.
21. Floyd A. Wyczalek, Tsih C. Wang, "*Electric Vehicle Regenerative Braking*", SAE P. 929139.
22. Christian Albrichsfeld, Juergen Karner, "*Regenerative Brake System for Hybrid and Electric Vehicles*", SAE P. 2009-01-1217.
23. Gino Sovran, Dwight A. Blaser, "*Quantifying the Potential Impacts of Regenerative Braking on a Vehicle's Tractive-Fuel Consumption for the U.S., European, and Japanese Driving Schedules*", SAE P. 2006-01-0664.
24. Michael Panagiotidis, George J. Delagrammatikas, Dennis N. Assanis, "*Development and Use of a Regenerative Braking Model for a Parallel Hybrid Electric Vehicle*", SAE P. 2000-01-0995.
25. Wittmer C., Dietrich P., Guzzella L., *Control Strategies for the ETH-Hybrid III Vehicle*, 1995, Proceedings First IFAC Workshop on Advances in Automotive Control.
26. Wittmer C., Guzzella L., Dietrich P., *Optimized Control Strategies for a Hybrid Car with a Heavy Flywheel*, 1996, Automatisierungstechnik, Vol. 7, pp. 331-337.
27. Guzzella L., Wittmer Ch., Ender M., *Optimal Operation of Drivetrains with SI-Engines and Fly-Wheels*, 1996, Proceedings of the 13th IFAC World Congress.
28. B. Vroemen, A. Serrarens, F. Veldpaus, *Hierarchical control of the Zero Inertia power train*, JSAE, 22(4), 2001.
29. Brockbank, C., "*Application of a variable drive to supercharger and turbo compunder applications*", SAE P. 2009-01-1465.
30. Brockbank, C., and Cross, D., "*Mechanical hybrid system comprising a flywheel and CVT for motorsport and mainstream automotive applications*", SAE P. 2009-01-1312.
31. Brockbank, C., and Greenwood, C., "*Fuel Economy Benefits of a Flywheel & CVT Based Mechanical Hybrid for City Bus and Commercial Vehicle Applications*", SAE P. 2009-01-2868.
32. Alberto Boretti, "*Comparison of fuel economies of high efficiency diesel and hydrogen engines powering a compact car with a flywheel based kinetic energy recovery systems*", International Journal of Hydrogen Energy (2010), doi:10.1016/j.ijhydene.2010.05.031.
33. Diego-Ayala, U., Martinez-Gonzalez, P., McGlashan, N. and Pullen, K., "*The mechanical hybrid vehicle: an investigation of a flywheel-based vehicular regenerative energy capture system*", Proc. IMechE Vol. 222 Part D: J. Automobile Engineering, pp. 2087-2101, 2008. doi: 10.1243/09544070jauto677.
34. <http://ricardo.com/Software/Products/WAVE/> (retrieved July 21, 2010).
35. <http://www.lesoft.co.uk/index1.html> (retrieved July 21, 2010).